Spectral and Thermal Mapping of Desert Surface Sediments for Agricultural Development

著者	KOCH Magaly, GABER Ahmed
journal or publication title	Journal of Integrated Field Science
volume	12
page range	73-77
year	2015-03
URL	http://hdl.handle.net/10097/60518

JIFS, 12 : 73 − 77 (2015) Oral Presentation

Spectral and Thermal Mapping of Desert Surface Sediments for Agricultural Development

Magaly KOCH[1] and Ahmed GABER[2]

[1]Center for Remote Sensing, Boston University, Boston, USA
[2]Geology Department, Faculty of Science, Port-Said University, Port-Said, Egypt

Abstract

A combination of multispectral, thermal and microwave data obtained from space and supported by ground measurements are used to investigate the surface sediment characteristics of a desert plain area in Egypt (El-Gallaba Plain, NW of Aswan). This plain once hosted an ancestral river system that is nowadays largely covered by aeolian and gravelly sands, and thus, only detectible with radar and thermal images. The methodology consists of extracting thermo-physical and textural parameters to guide and improve supervised spectral classification results. The results show that surface mineralogy (obtained from spectral information) correlates strongly with surface emissivity, whereas grain size and surface roughness strongly correlates with apparent thermal inertia. Furthermore, several broad strips of thermal cooling-anomalies are arranged in a linear fashion and diagonally crossing the alluvial basin. The sediments within these strips show very different textural, thermo-physical and compositional characteristics with respect to the surrounding areas suggesting that they were deposited under different depositional environments such as structurally controlled linear basins. These tectonic depressions were confirmed by ground penetrating radar and could be promising areas for groundwater accumulation and exploration enabling agricultural development in the El-Gallaba Plain of the Western Desert in Egypt.

Introduction

The aim of this work is to determine to what extent multisensor satellite data (operating in the optical, thermal, microwave spectral region) can be used to characterize and map desert surface sediments in an effort to aid soil and water resources exploration for land use planning. Such planning efforts are aimed to reclaim desert land for agricultural use in order to cope with increasing food and water demands for a growing population. The implementation of large agricultural activities in desert environments requires detailed knowledge about the soil and water characteristics, quality and availability. However such information is often incomplete or nonexistent, as for example in the *El-Gallaba Plain*, located northwest of Aswan in the Western Desert of Egypt. This is a desert plain area that contains a large fluvial fan (30 x 60 km^2) from an ancestral river system that was once active long before the river Nile even existed. Nowadays the fluvial deposits are largely covered by aeolian and gravelly sands and thus mostly detectible with radar and thermal images. The El-Gallaba basin has been subject of past and present-day research with respect to its deltaic and fluvial deposits and complex tectono-geomorphic history (Hinz et al., 1993; Thurmond et al., 2004; Gaber et al., 2011; Roden et al., 2011).

The methodology presented in this work consists of (1) processing multi-spectral, thermal (ASTER) and microwave (RADARSAT-2) data for identifying main surface covers, especially gravelly (fluvial) soils, and migrating sand dunes / sand sheets, (2) extracting thermo-physical (kinetic surface temperature, emissivity, and thermal inertia) and textural properties (grain size, surface roughness), (3) correlating surface mineralogy with textural and thermal properties, and (4) validating satellite-derived products with field observation and measurements (ground penetrating radar GPR).

Thermal Surface Material Mapping

Desert surface materials can be characterized through a combination of thermo-physical data (e.g. albedo and thermal inertia) and mineralogy. Studies have shown that for instance dust, duricrust and rocks show very characteristic combinations of albedo and thermal inertia that enable mapping their distribution even in planetary environments such as Mars (Jones et al., 2014). Furthermore, when desert surfaces are covered by a thin layer of dust and sand, thermal properties of the underlying consolidated layers may be detectable by thermal sensors, providing geologist with a valuable mapping tool (Kahle et al., 1976). Such thermal properties are emissivity, radiant temperature and thermal inertia, which are used to describe the behavior of materials to heat radiation (Sabins, 1997).

Thermal inertia (TI) is a measure of the ability of a material to store and conduct heat, and correlates strongly with material density, particle size and degree of cementation. In other words, TI measures the resistance of a material to changes in temperature. It is possible to estimate TI from space only indirectly by using a model. Thus the inferred parameter is called apparent thermal inertia (ATI) and is a unit less value (Cracknell and Xue, 1996). ATI is computed from surface albedo and diurnal temperature differences, which means that ideally minimum and maximum surface temperature should be known. This limits its estimation to a few satellite sensors such as MODIS and ASTER. Emissivity on the other hand is a measure of the ability of a material to absorb and radiate incident solar radiation, and is dependent on the chemical composition of the material. This property is often used for surface mineralogy mapping.

For our study area we searched for ASTER thermal pairs (day and night images) that would be as close in time as possible. However for most geological applications ATI can be estimated with sufficient accuracy if image pairs are acquired within a period of a few days or weeks (Kahle and Alley, 1985). We therefore selected two ASTER thermal images acquired on 6th (night) and 28th (day) of January 2011 to calculate the thermal parameters. However, in order to calculate the albedo all ASTER reflective bands are required as this parameter is a measure of the fraction of incident visible to near infrared radiation reflected by the surface. Thus an image of February 5th, 2008 (representing the same season) was selected due to the fact that ASTER's SWIR detectors stopped working shortly after that date.

The thermal bands processing consisted of (1) converting AST-09T product to thermal radiance, (2) running an atmospheric correction, (3) calculating kinetic surface temperature, (4) extracting surface emissivity by applying the emissivity normalized method in ENVI, and (5) estimating ATI using the equation $\frac{1-A}{\Delta T}$, where A is albedo and ΔT is the day-night temperature difference.

Albedo and emissivity are two parameters that are positively correlated and related to mineralogy. A 2-D scatterplot showing this relationship was used to threshold the emissivity map into main desert surface units (rock outcrops, alluvial fans, gravelly and sandy surfaces). This step allowed classifying the study area into main thermo-physical units that were used in a later step to extract and locate endmember spectra for individual units.

The variation of thermal inertia is inversely proportional to surface temperature (day – night) differences (Fig. 1) and can be related to lithologic units. Surface materials with low ATI rapidly heat during

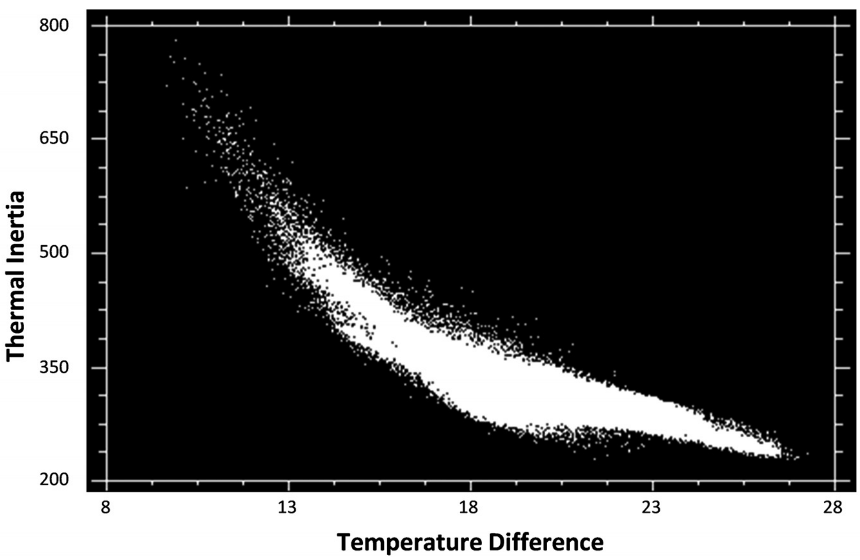

Figure 1. Linear relationship between thermal inertia and day/night temperature difference.

the day and cool during the night. An example of this behavior is loose drift sand. The opposite are dense (and dark) materials with high ATI such as bedrock outcrops covered with desert varnish (causing a darkening effect on the surface). The ATI and emissivity maps were compared in a later step to surface mineralogy and surface roughness in order to infer subsurface geological structures that are not visible on optical images alone.

Spectral Surface Material Mapping

Spectral classification was performed on all nine reflective bands of ASTER. Therefore an image of 5th of February 2008 was selected to avoid the problem with the SWIR radiometer failure that occurred in April 2008. Unfortunately no day-night thermal pair was acquired during that time, so the thermo-physical properties had to be extracted from a later ASTER image pair (January 2011). It was assumed that desert environmental conditions were quite similar during both image acquisitions.

The thermo-physical units that were obtained from the albedo-emissivity relationship described in the previous section constituted the basis for extracting endmembers representing different surface materials. The Sequential Maximum Angle Convex Cone (SMACC) spectral tool (available in ENVI) was used to find endmembers of pure surface materials per thermo-physical unit. A total of eight units were individually searched for endmembers resulting in eight representative spectral curves. The endmembers and their locations were visually inspected and compared to Google Earth images and field photos whenever available. Furthermore, the endmembers were matched against a set of ASTER spectral libraries (http://speclib.jpl.nasa.gov/) in order to determine their true identity.

Once the identity of the spectra was established, a supervised Spectral Angle Mapping (SAM) classification was performed using the eight endmembers as reference vectors and a similarity angle of 0.1 radians. This resulted in a classified image with the following class labels: class1 (sandstone), class 2 (limestone), class 3 (calcareous gravel), class 4 (marl/shale), class 5 (drift sand), class 6 (calcareous tufa), class 7 (shadows/water), and class 8 (gravel/flint).

Correlation of Surface Material with Thermal and Radar Properties

The application of SAM classification to map surface constituents (mineralogy) using reference vectors derived with the aid of thermo-physical units was further explored by running a set of zonal statistical measures in ArcGIS. For each SAM class (except class 7 shadow/water) the mean emissivity and standard deviation was calculated (Table 1). The results confirm that emissivity relates to the composition of the surface showing generally higher values for dense rocky surfaces (class 1 = sandstone, and class 2 = limestone) and lower values for loose grainy surfaces (class 5 = drift sand, and class 8 = gravel/flint).

To further explore the relationship between grain size (or rock fragmentation) and surface sediment type, RADARSAT-2 full polarimetric data were processed to obtain three sets of parameters describing the predominant SAR scattering mechanism: alpha angle which is associated with the type of dominant scattering mechanism, entropy which is a measure of scattering randomness, and anisotropy which describes whether one or several scattering phenomena coexist. Table 2 summarizes this relationship and confirms that the smoothest surfaces are the nearly flat sandstone peneplain (class 1), and the sandy (class 5) and gravelly (class 8) plains of El-Gallaba. In addition, supervised classification of the full polarimetric radar data was performed to further classify the El-

Table 1. Correlation of spectral classes and emissivity.

Sedimentary Classes	Emissivity 2008	
	Mean	**STD**
Class 1	0.813112	0.028543
Class 2	0.917156	0.012801
Class 3	0.879791	0.036844
Class 4	0.85161	0.032497
Class 5	0.794511	0.028276
Class 6	0.899818	0.022294
Class 8	0.795379	0.02419

Table 2. Correlation of spectral classes and radar scattering mechanism.

Sedimentary Classes	SAR Scattering Mechanism (Mean)		
	Alpha	Entropy	Anisotropy
Class 1	10.667876	0.276344	0.122423
Class 2	16.97365	0.397083	0.056789
Class 3	17.359285	0.428084	0.085935
Class 4	15.815497	0.406366	0.120726
Class 5	11.552115	0.314189	0.283767
Class 6	17.989788	0.461051	0.185498
Class 8	11.960143	0.321885	0.253435

Gallaba plain sediments into five classes, namely two gravel classes, two mixtures of gravel and sand, and one sand class. The resulting classes were compared to the ATI map and the ATI mean/std. per class was computed. The gravels show generally higher thermal inertia than the loose drift sand (Table 3).

Moreover, the sandy and gravelly surfaces of El Gallaba Plain enclose a very interesting thermal phenomenon that appears especially obvious on the emissivity map (Fig. 2). Several broad strips of thermal cooling anomalies appear arranged in a linear fashion and diagonally crossing the desert basin. Variations

Table 3. Correlation of radar classes and apparent thermal inertia.

Sedimentary Classes	Apparent Thermal Inertia (ATI)	
	Mean	STD
Gravel-1	331.28165	19.265427
Gravel-2	319.21512	27.982611
Gravel/Sand-1	315.40887	17.431963
Gravel/Sand-2	311.52066	22.307337
Sand	309.74426	16.990351

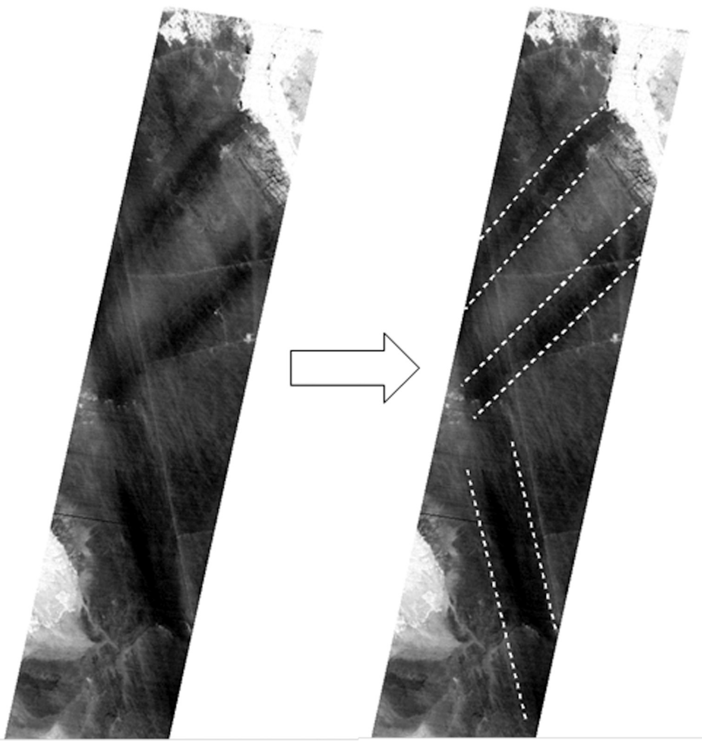

Figure 2. Thermal anomalies indicating possible sedimentary block boundaries.

in emissivity values seem to respond to lithological boundaries and/or tectonic disturbances, and thus, seem to mark fault zones delimiting dropped blocks. The sediments within these strips show very different textural, thermo-physical and compositional characteristics with respect to the surrounding areas suggesting that they were deposited under different depositional environments such as structurally controlled linear basins.

Field surveys using ground penetrating radar (GPR) were run across the thermal boundaries to confirm the nature of these anomalies. The GPR profiles reveal obvious offsets in the subsurface stratigraphy suggesting the presence of highly fractured zones flanking the thermal anomaly strips. This strongly suggests the existence of graben-like structures. The detected buried channels and/or depositional environments and faults may well form good groundwater traps or recharge conduits. Consequently, the structurally controlled El-Gallaba Plain basin could be a promising area for groundwater accumulation and exploration enabling much needed agricultural expansion west of the Nile.

Conclusion

The integration of multisensor data (optical, thermal, microwave) shows promising results in terms of mapping desert surface lithology and near surface features such as fault zones or paleochannels covered by a thin layer of sands and gravels. Surface mineralogy seems to be strongly related to emissivity whereas grain size seems to correlate best with apparent thermal inertia (ATI). Being able to map gravel content, size, and type from space opens up an important mapping tool for determining suitability of soils for irrigated agriculture in areas where detailed soil maps are lacking. Another potential application of this mapping tool is to determine the relative age of gravelly surfaces by detecting their smoothness or roughness and their coating (desert varnish). This would allow drawing valuable conclusions about the paleo-environmental history of desert fluvial landscapes.

Acknowledgement

The authors would like to thank the USGS Earth Resources Observation and Science (EROS) Center for providing the ASTER data, and the Canadian Space Agency (CSA) and MDA for providing the RADARSAT-2 data as part of the SOAR-EI project no. 5138.

References

Cracknell, A.P., and Y., Xue (1996) Thermal Inertia Determination from Space – A Tutorial Review. Int. J. Remote Sensing, 17 (3): 431-461.

Gaber, A., M., Koch, M.H., Geriesh and M. Sato (2011) SAR Remote Sensing of Buried Faults: Implications for Groundwater Exploration in the Western Desert of Egypt. Sensing and Imaging: An International Journal, 12 (3-4): 133-151.

Hinz, E.A., R.J., Stern, A.K., Thurmond, M.G., Abdelsalam and M.M., Abdeen (2003) When did the Nile begin?: Remote sensing analysis of paleodrainages near Kom Ombo, Upper Egypt. American Geophysical Union, Fall Meeting, Abstract #H52A-1182, San Francisco, CA, USA.

Jones, E., G., Caprarelli, F.P., Mills, B., Doran and J., Clarke (2014) An Alternative Approach to Mapping Thermophysical Units from Martian Thermal Inertia and Albedo Data Using a Combination of Unsupervised Classification Techniques. Remote Sensing, 6: 5184-5237.

Kahle, A.B. and R.E., Alley (1985) Calculation of Thermal Inertia from Day-Night Measurements Separated by Days or Weeks. Photogrammetric Engineering and Remote Sensing, 51 (1): 73-75.

Kahle, A.B., A.R., Gillespie and A.F.H., Goetz (1976) Thermal Inertia Imaging: A New Geologic Mapping Tool. Geophysical Research Letters, 3 (1): 26-28.

Roden, J., M.G., Abdelsalam, E., Atekwana, G., El-Qady and E.A., Tarabees (2011) Structural influence on the evolution of the pre-Eonile drainage system of southern Egypt: Insights from magnetotelluric and gravity data. Journal of African Earth Sciences, 61: 358-368.

Sabins, F.F. (1997) In Remote Sensing: Principles and Interpretation. 3rd edition, Floyd F. Sabins (ed.), p. 494, W.H. Freeman and Co., New York

Thurmond, A.K., R.J., Stern, M.G., Abdelsalam, K.C., Nielsen, M.M., Abdeen and E., Hinz (2004) The Nubian Swell. Journal of African Earth Sciences, 39: 401-407.